

# A virtual octane test simulator for gasoline/ethanol blends

Andrew Smallbone<sup>2</sup>, RCR Shaw<sup>1</sup>, Neal Morgan<sup>3</sup> and Markus Kraft<sup>1</sup>

released: 09 January 2012

<sup>1</sup> Department of Chemical Engineering  
and Biotechnology  
University of Cambridge  
New Museums Site  
Pembroke Street  
Cambridge, CB2 3RA  
United Kingdom  
E-mail: [mk306@cam.ac.uk](mailto:mk306@cam.ac.uk)

<sup>2</sup> cmcl innovations  
Sheraton House  
Castle Park  
Cambridge, CB3 0XR  
United Kingdom  
E-mail: [ajsmallbone@cmclinnovations.com](mailto:ajsmallbone@cmclinnovations.com)

<sup>3</sup> Shell Global Solutions Chester  
E-mail: [mk306@cam.ac.uk](mailto:mk306@cam.ac.uk)

Preprint No. 111



**Edited by**

Computational Modelling Group  
Department of Chemical Engineering and Biotechnology  
University of Cambridge  
New Museums Site  
Pembroke Street  
Cambridge CB2 3RA  
United Kingdom

**Fax:** + 44 (0)1223 334796

**E-Mail:** [c4e@cam.ac.uk](mailto:c4e@cam.ac.uk)

**World Wide Web:** <http://como.ceb.cam.ac.uk/>



## **Abstract**

This work describes the development of a quaternary component chemical kinetic gasoline fuel model and its validation in context with shock tubes experiments and Spark Ignition (SI) engines. The model contains oxidation chemistry for Toluene, n-Heptane, Ethanol, and iso-Octane (THEO), as well as sub-mechanisms for simulating the formation of regulated  $\text{NO}_x$  and soot precursor emissions. A virtual octane test simulator was also developed to model new experimental data obtained in Research Octane Number (RON) tests, for the first time results were used to benchmark chemical kinetic mechanism performance in a practical engine context with respect to other state-of-the-art detailed and comprehensive fuel models.

# Contents

<b>1</b>	<b>Introduction</b>	<b>3</b>
<b>2</b>	<b>Development of a THEO fuel model</b>	<b>3</b>
2.1	Fuel model optimisation . . . . .	5
2.2	Shock Tube Comparisons . . . . .	6
<b>3</b>	<b>Engine Simulations</b>	<b>7</b>
3.1	Engine Simulator . . . . .	7
3.2	Knocking S.I. combustion mode . . . . .	9
3.3	ASME Research Octane Number test . . . . .	9
3.3.1	Simulation method . . . . .	9
3.3.2	Other fuel models . . . . .	11
<b>4</b>	<b>Discussion</b>	<b>12</b>
<b>5</b>	<b>Summary</b>	<b>12</b>
	<b>References</b>	<b>13</b>

# 1 Introduction

Ethanol is a simple and abundant biofuel that can be blended with traditional gasoline to potentially lower the net carbon dioxide emissions from the transportation sector [24].

The addition of ethanol to standard gasoline impacts engine performance, most notably engine knock [16], which is quantified using the standard research and motor octane test methods [3][4]. Hence as bio-fuel component fractions increase, engineers must find ways to exploit the advantages of these fuels through improved engine design.

A major tool used in the development of modern IC engines is computational simulation. Recent advancements in chemical kinetics have improved model robustness in terms of simulating fuel combustion and regulated emissions characteristics, thus enabling a greater number of design iterations to be carried out on the desktop. Conventionally, computational modeling of fuel oxidation and emissions formation in IC engines has been limited to bi-component (n-heptane and iso-octane)[10] and simplified fuel models suitable for the CPU times associated with 3D computational fluid dynamics (CFD) [7]. In recent years, advancements into more detailed tri-component [1][23](toluene, n-heptane, and iso-octane) fuel models have improved relevance to practical fuels [20], mainly through increased scope in terms of fuel sensitivity. The adoption of these models have remained computationally efficient through the utilization of Stochastic Reactor Model (SRM)-based engine simulation approaches [21] [20], which solve for engine processes using a probability density function (PDF) based method [25].

This paper presents the development of a quad-component chemical kinetic fuel model for toluene, n-heptane, ethanol, and iso-octane (THEO) fuel blends ready for direct application to IC engine simulations of practical fuels blended with bio-fuel components. Semi-detailed sub-mechanisms for  $\text{NO}_x$  and soot (PM) formation have been retained [22] such that the simulations can model key mandated exhaust gas emission performance indicators. This model is validated against experimental data obtained from shock tubes, jet-stirred reactors, and engine experiments of spark ignition (SI) knocking combustion for various THEO blends. A method to simulate the Research Octane Number (RON) test is presented such that fuel model performance can be assessed with respect to a well established engine performance metric. The same method is applied to a set of representative fuel models of semi-detailed [5], detailed [23] and comprehensive size [9], and their performances are compared.

## 2 Development of a THEO fuel model

The chemical kinetic mechanism, THEO, was developed in three main stages. An outline of the process employed is presented in Figure 1.

A Toluene Reference Fuel (TRF) mechanism reported by Andrae *et al.* [2] has been used in previous work for simulating a surrogate for gasoline [20]. These authors extended

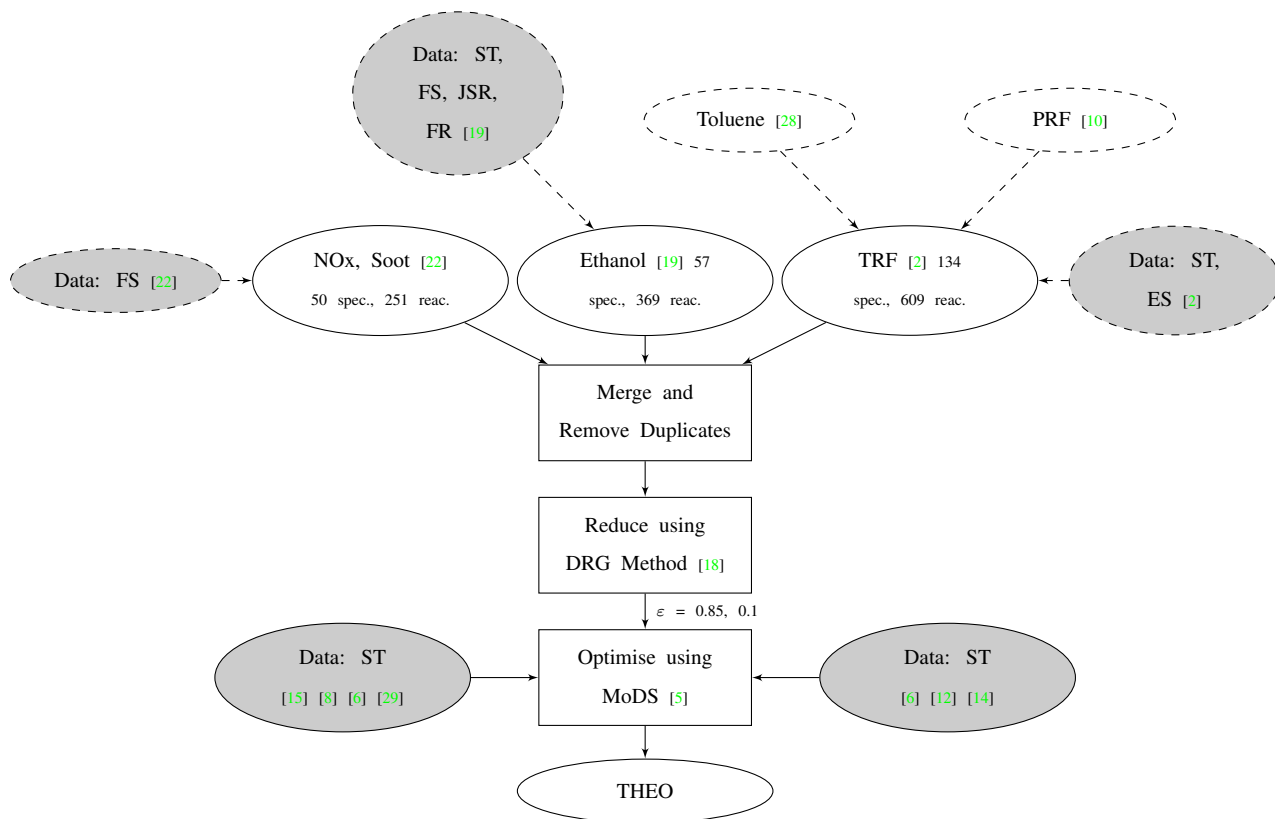


**Figure 1:** Mechanism map for THEO development. Abbreviations are: ST=Shock Tube, FS = Flame Speed, JSR = Jet-Stirred Reactor, FR = Flow Reactor and ES = Engine Simulation.

a comprehensive Primary Reference Fuel (PRF) submechanism [9] containing n-heptane and iso-octane oxidation chemistry by including a toluene submechanism reported by Sivamarakrishnan *et al.* [27]. In the work presented here, this TRF mechanism was further extended to include an ethanol oxidation sub-mechanism [19] together with NO<sub>x</sub> and soot precursor chemistry [22].

A reduction of the extended mechanism was performed using the Directed Relation Graphing (DRG) method proposed by Lu and Law [18]. The reduction process proved more challenging due to the inclusion of NO<sub>x</sub> and soot precursor chemistry which both have minimal impact on the oxidation-based metrics employed in DRG techniques. Hence the reduction was performed without the NO<sub>x</sub> and soot precursor chemistry, after the reduction these submechanisms were re-added.

The reduction was carried out twice using the intermediate mechanism to minimize error propagation. Sample results demonstrating the robustness of the reduction are presented in Figure 2 for OH concentrations in a 0D batch reactor, the reduced mechanism proved satisfactorily accurate over engine-relevant ranges of pressures, temperatures, and equivalence ratios.

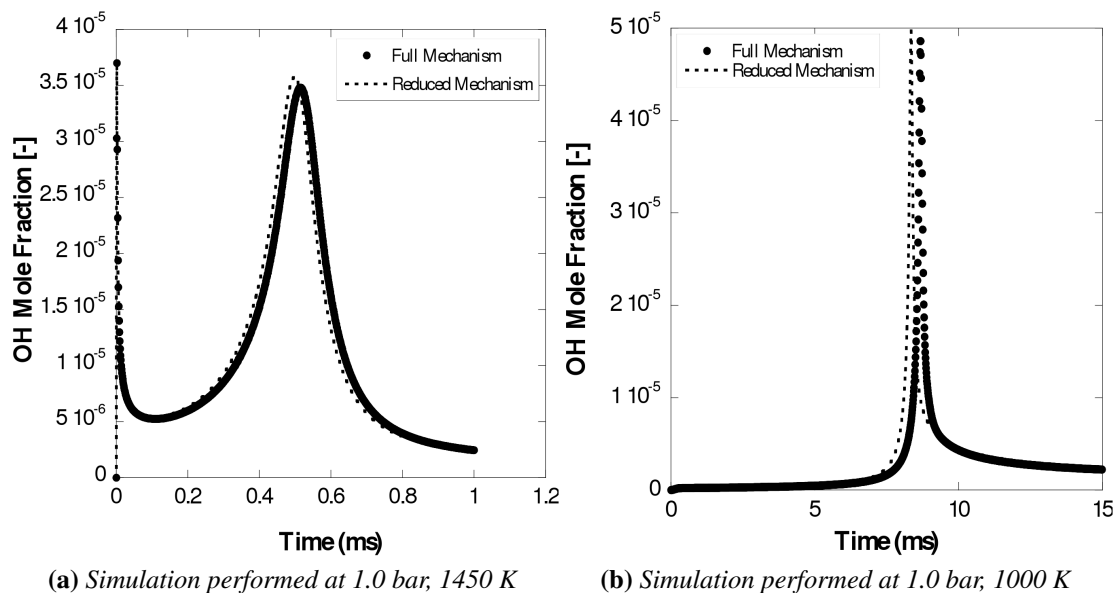


**Figure 2:** Sample of the results in the comparison between full and skeletal mechanisms for a stoichiometric mixture of 85.0% (mol.) AR, 10.0% O<sub>2</sub>, 0.1% C<sub>2</sub>H<sub>5</sub>OH, 0.9% C<sub>6</sub>H<sub>5</sub>CH<sub>3</sub>, 3.0% C<sub>7</sub>H<sub>16</sub>, and 1.0% C<sub>8</sub>H<sub>18</sub> mixture.

## 2.1 Fuel model optimisation

The reduced mechanism was optimized with respect to experimental data using the Model Development Suite (MoDS) with detailed methods outlined previously [5]. This tool enables the differences between the model and experimental responses to be quantified and minimized using an objective function similar to the one employed by Sheen *et al.*

[26]:

$$\Phi_1(x) = \sum_{i=1}^N \sum_{j=1}^{M_i} [\eta_{ij}^{exp} - \eta_{ij}(x)] \quad (1)$$

where  $\eta_{ij}(x)$  is the model response to a set of model parameter  $x$ , and  $\eta_{ij}^{exp}$  is the experimental data corresponding to  $x$ . A low discrepancy Sobol sequence [30] is used to perform a global search to identify the global minimum of the objective function.

Ignition delay times obtained using shock tubes were identified as the base parameters for optimization. Table 1 gives an overview of the data sets used and their corresponding conditions. The mechanism was optimized against over one hundred experimental data points from six independent sets of experiments. The reactions modified during the optimization are listed in Table 2; the pre-exponential Arrhenius coefficient,  $A$ , as well as the reaction activation energy,  $E_a$ , were optimized within their expected ranges of uncertainty.

**Table 1:** Summary of experimental data sets;  $\Phi = 1.0$

Temp. Range (K)	Pressure (bar)	Fuel	Reference
1358 - 1758	3.039	$C_6H_5CH_3$	[6]
1150.5 - 1528.1	3.5	$C_2H_5OH$	[12]
720 - 1232	16.8 - 55.6	$C_2H_5OH, C_8H_{18}, C_7H_{16}$	[14]
859 - 1137	16.1 - 52.8	$C_6H_5CH_3, C_8H_{18}, C_7H_{16}$	[15]
764 - 1201	9.9 - 51	$C_6H_5CH_3, C_2H_5OH, C_8H_{18}, C_7H_{16}$	[8]
1136.7 - 1376	4.356	$C_8H_{18}$	[6]
1367.8 - 1631.1	1.0	$C_7H_{16}$	[29]

## 2.2 Shock Tube Comparisons

The optimized mechanism was compared against both the non-optimized mechanism and experimental data points. Associated experimental errors were estimated using typical reported spatial/temporal variations and measurement apparatus [29][11] errors.

Sample sets of test data are presented Figures 3 and 4, in both cases these show that the optimization has been successful with minimized differences between observed model responses and experimental measurement. The model was significantly improved at 30 and 50 bar, as seen in Figures 4a and 4b. The derived mechanism was considered of sufficient robustness for further application to IC engines.



**Table 2:** Summary of the optimised reactions

Reaction
$O + OH \rightleftharpoons O_2 + H$
$O + HO_2 \rightleftharpoons O_2 + OH$
$H + OH + M \rightleftharpoons H_2O + M$
$HO_2 + HO_2 \rightleftharpoons H_2O_2 + O_2$
$C_2H_5OH + OH \rightleftharpoons CH_3CHOH + H_2O$
$C_2H_5OH + OH \rightleftharpoons CH_3CH_2O + H_2O$
$C_2H_5OH + H \rightleftharpoons C_2H_4OH + H_2$
$C_6H_5CH_3 + OH \rightleftharpoons C_6H_5CH_2 + H_2O$
$C_6H_5CHO + O_2 \rightleftharpoons C_6H_5CO + HO_2$
$C_7H_{16} \rightarrow PC_4H_9 + IC_3H_7$
$C_7H_{16} + O_2 \rightarrow C_7H_{15-2} + HO_2$
$C_7H_{16} + OH \rightarrow C_7H_{15-2} + H_2O$
$C_7H_{15-2} + O_2 \rightarrow C_7H_{15}O_2$
$C_7H_{16} + H \rightarrow C_7H_{15-1} + H_2$
$C_8H_{18} + HO_2 \rightleftharpoons AC_8H_{17} + H_2O_2$

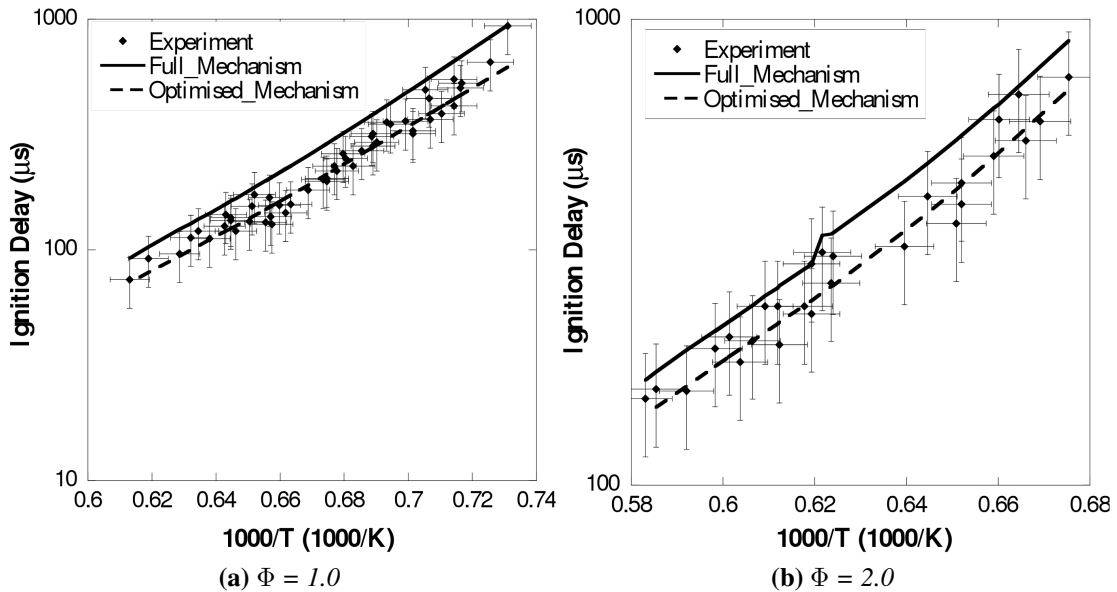


**Figure 3:** *N*-heptane ignition delay time comparisons[29]

## 3 Engine Simulations

### 3.1 Engine Simulator

The SRM [17] is derived from more general PDF transport models [25]. It is a zero dimensional model with assumed statistical homogeneity. This assumption is of funda-

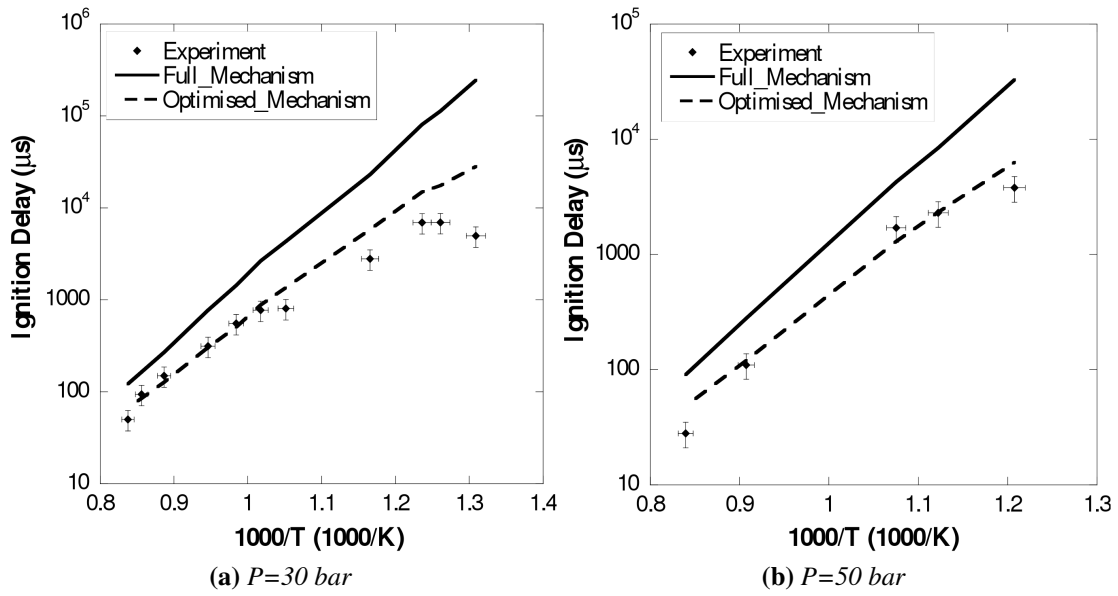


**Figure 4:** Blends of *n*-heptane, iso-octane, ethanol and toluene from Cancino et al. [8].

mental importance to delivering robust computations of heat release rates and emissions where inhomogeneities are critical, particularly in the mixture composition and thermal domains. The model is solved by adopting a user-defined number of stochastic particles that represent the PDF. The SRM employed in this study is outlined comprehensively including a detailed mathematical description in papers [17] [13] [20].

In this work, spark ignition combustion subroutines presented previously [13] have been further developed and simplified from a three-zone to a two-zone approach suitable for knocking combustion applications. This was carried out through the implementation of an advanced operator splitting routine such that flame propagation could be simulated with minimal stochastic noise for reduced numbers of particles, thus minimizing CPU times whilst retaining adequate model robustness.

The specifications of the apparatus employed in the engine validation phase are outlined in Table 3.

**Table 3:** Engine Specifications

	units	LUPOE	CFR
bore	mm	80.0	85.2
stroke	mm	74.0	112.0
con-rod	mm	148.0	254.0
C.R.	-	17.6	variable
Engine speed	RPM	1500	600
spark timing	CAD bTDC	20.0	13.0
inlet pressure	bar	1.08	1.00
inlet temperature	K	343.0	325.0

## 3.2 Knocking S.I. combustion mode

The experimental data obtained in a knocking spark ignition engine [7] were employed to test the performance of the mechanism in an IC engine context. This engine was operated at the condition outlined in Table 3. Presented in Figure 5 are the corresponding pressure-crank angle histories for a typical cycle with mean knock onset times for both the model and experiment. Simulated knock onset times proved to be within observed experimental repeatability for the i-octane and n-heptane blends.

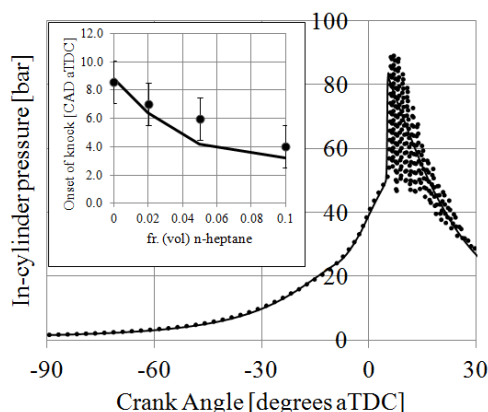


**Figure 5:** *In-cylinder P-CAD profile of a stoichiometric 90:10 i-octane:n-heptane blend, together with mean knock onset times for various i-octane/n-heptane blends.*

## 3.3 ASME Research Octane Number test

The Research Octane test method [4] is an engineering metric intended to measure the resistance of a particular fuel to knock in IC engines. Its application has been extensively documented throughout the history of IC engine and fuel development [16]. Whilst experimental octane number data are widely available for pure component fuels [16], due to reasons such as commercial confidentiality and reluctance to modify standard test apparatus, comprehensive data sets for even common hydrocarbon blends, in-cylinder pressure etc. remain sparse [31]. However experimental data from RON tests for tri-component blends have been presented by the authors previously [20, 21]. In this study the data set was further extended to twenty-two measurements with the addition of ethanol blends.

### 3.3.1 Simulation method

In addition to employing the test procedure outlined in the standard test documentation [4], a few additional assumptions were made to reduce the number of permutations required to carry out the simulation.

1. Peak knock intensity was assumed to occur with an equivalence ratio of 1.05 (rather than identified by running the engine over the full range of equivalence ratios).

2. The turbulent flame propagation rate was considered independent of fuel (previous experimental analysis has demonstrated that this could vary by as much as 10-20% [7] [31])
3. The Critical Compression Ratio (C.C.R.) was assumed to be obtained when the maximum rate of pressure rise occurred at 12.5 CAD aTDC.

The simulator was operated using fifteen stochastic particles, with the boundary conditions set according to the standard test procedure [4] and those in Table 3. The flame propagation sub-models were parameterized using the in-cylinder pressure and heat release rate data from [31]; a sample of the comparison of typical in-cylinder pressure-crank angle results are presented in Figure 6. In this case, the heat release prior to knock is reproduced sufficiently along with the rate of heat release once autoignition has occurred.

In order to identify the C.C.R., the compression ratio was increased by increments of 0.1, with typical model responses presented in Figure 7b as a function of compression ratio. The definition of a "knocking" engine is generally considered a subjective assessment [16], with the standard test employing a knock intensity meter or historically "a highly trained engineer". The requirement for standardizing the definition of knock is notable as knock occurred with increasing severity from a compression ratio of 5.6 and upwards. In this work, the authors attempted to define knock using various definitions of knock intensity and knock onset times; however, once a definition was imposed across the analysis, these yielded similar performance trends to the adopted Assumption 3.

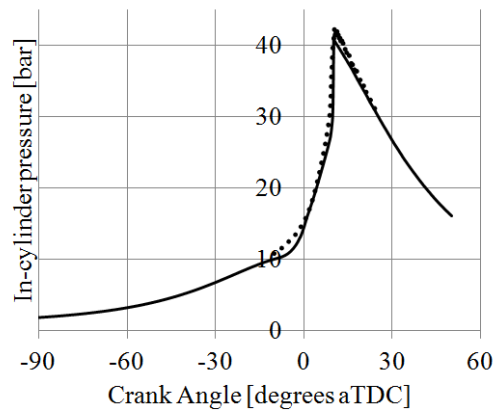
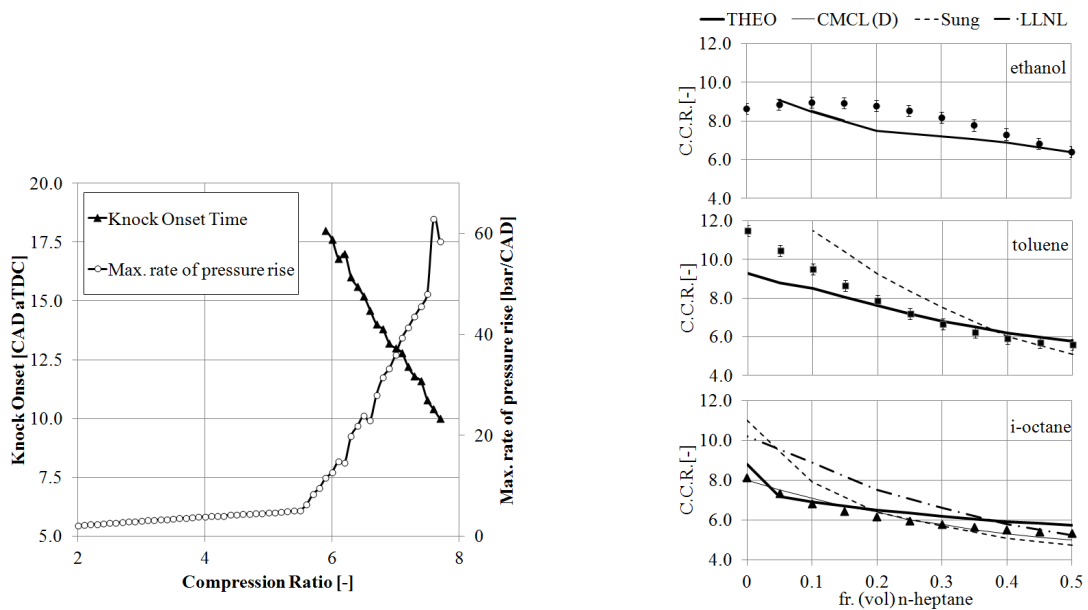


**Figure 6:** *In-cylinder pressure-crank angle profile of a sample 90:10 i-octane:n-heptane blend.*

Presented in Figure 7b are corresponding experimental and simulated C.C.R. data for the THEO mechanism in various blends of n-heptane and i-octane, toluene or ethanol. Computed ratios generally proved accurate to within 1.0 for the i-octane blends, to within 0.5 (other than for n-heptane liquid volume fractions of less than 0.1) for toluene and 1.5 for ethanol. Across all three data sets, results were considered in good agreement with experiments. The non-linear blending noted in the ethanol/n-heptane blends was not mimicked in the model, suggesting that additional crossover reactions may be required



(a) In-cylinder maximum  $dp/dCAD$  and knock onset times as a function of compression ratio

(b) Experimental and Computed Critical Compression Ratios

**Figure 7:** Simulations of the RON test [4]

in future developments. In addition, since in-cylinder pressure data was not available for the toluene and ethanol blends, further refinement for simulating flame propagation could improve model performance for the lower n-heptane concentrations in both toluene and ethanol.

### 3.3.2 Other fuel models

To benchmark the performance of the THEO mechanism, the same exercise was carried out using other representative mechanisms. These are summarized in Table 4, with results presented in Figure 7b.

**Table 4:** Summary of the fuel models tested

Name	tol	eth	n-hep	i-oct	NO <sub>x</sub> , soot	no. species	no. react	CPU* (min)
THEO [this paper]	✓	✓	✓	✓	✓	163	1012	3.8
CMCL(D) [22]	✓	✓	✓	✓	✓	208	1002	4.5
Sung [23]	✓	✗	✓	✓	✗	386	1591	20
LLNL [9]	✗	✗	✓	✓	✗	1034	4236	725

\* CPU time for a single engine cycle run on one processor

The following observations were made: a) in an engine context there was no direct link between mechanism size/CPU time and model performance, b) the CMCL(D) [22] mech-

anism proved most robust for i-octane/n-heptane blends, c) the largest mechanism (LLNL) [9] was not sensitive enough to ignition at low n-heptane concentrations, and d) the THEO mechanism proved most robust for the i-octane and toluene blends compared to the Sung [23] mechanism.

## 4 Discussion

For the first time, a method for simulating the ASME RON test is presented. This enables engineers to formally assess chemical kinetic mechanism performance in the context of well established, standardized, industry reliant experimental test data. Through the adoption of these methods, engineers can make an informed decisions for which mechanism to employ for their particular application. The performance of detailed and even comprehensive chemical kinetics mechanisms has demonstrated no clear link between mechanism size, CPU time and robustness in an IC engine context. This observation highlights two key points: i) the importance of considering more IC engine data in the development of such mechanisms, this work has demonstrated methods to facilitate this process and, ii) the sensitivity of the mechanism to the experimental data considered during its development, and thus a need to employ more advanced and systematic optimization approaches [5] such as those presented here.

A novel chemical kinetic mechanism including  $\text{NO}_x$  and soot chemistry for bio-fuel/gasoline blends has been developed which can be applied directly to practical engine design using SRM-based and other low CPU intensive engine simulators. This enables for development engineers to expand their analysis from simple bi-component gasoline fuel surrogates to those with fuel sensitivity and bio-fuel components, in addition engineers will be able to analyze their technologies in terms of key legislated exhaust gas emissions.

## 5 Summary

The development of a novel THEO chemical kinetic mechanism for gasoline and bio-fuel blends consisting of n-heptane, iso-octane, toluene, and ethanol with  $\text{NO}_x$  and soot chemistry was completed and results presented.

The performance of the mechanism was then assessed in an IC engine context by simulating knock in a spark ignition research engine and by developing a method to simulate the standard ASME RON test. Using new RON test data for THEO blends, the fuel model was tested with respect to octane test data. The THEO mechanism proved the most robust when compared to a variety of alternative detailed chemical kinetic mechanisms of varying size and detail.

## References

- [1] J. Andrae and R. Head. Hcci experiments with gasoline surrogate fuels modeled by a semidetailed chemical kinetic model. *Combustion and Flame*, 156:842 – 851, 2009.
- [2] J. Andrae, P. Pjornbom, R. Cracknell, and G. Kalghatgi. Autoignition of toluene reference fuels at high pressures modeled with detailed chemical kinetics. *Combustion and Flame*, 149:2 – 24, 2007.
- [3] ANSI. Standard test method for motor octane number of spark-ignition engine fuel. Technical Report D2700-08, ASTM, .
- [4] ANSI. Standard test method for research octane number of spark-ignition engine fuel. Technical Report D2699-08, ASTM, .
- [5] G. Brownbridge, A. Smallbone, W. Phadungsukanan, S. Mosbach, M. Kraft, and B. Johansson. Automated ic engine model development with uncertainty propagation. SAE Paper No. 2011-01-0237, 2011.
- [6] A. Burcat, R. Farmer, R. Espinoza, and R. Matula. Comparative ignition delay times for selected ring-structured hydrocarbons. *Combustion and Flame*, 36:313 – 316, 1979.
- [7] A. Burluka, K. Liu, C. Sheppard, A. J. Smallbone, and W. R. The influence of simulated residual and NO concentrations on knock onset for PRFs and gasolines. SAE Paper No. 2004-01-2998, 2004.
- [8] L. Cancino, M. Fikri, A. Oliveira, and C. Schulz. Autoignition of gasoline surrogate mixtures at intermediate temperatures and high pressures: Experimental and numerical approaches. *Proceedings of the Combustion Institute*, 32:501 – 508, 2009.
- [9] H. Curran, P. Gaffuri, W. Pitz, and C. Westbrook. A comprehensive modeling study of iso-octane. *Combustion and Flame*, 129:3:253–280, 2002.
- [10] H. J. Curran, P. Gaffuri, W. J. Pitz, and C. K. Westbrook. A comprehensive modeling study of iso-octane oxidation. *Combust. Flame*, 129:253–280, 2002.
- [11] D. Davison and R. Hanson. Interpreting shock tube ignition data. *International Journal of Chemical Kinetics*, 36:510 – 523, 2004.
- [12] M. Dunphy and J. Simmie. High-temperature oxidation of ethanol. *Journal Chemistry Society, Faraday Trans.*, 87:1691 – 1696, 1991.
- [13] J. Etheridge, S. Mosbach, M. Kraft, H. Wu, and N. Collings. Modelling soot formation in a disi engine. *Proceedings of the Combustion Institute*, 33:3159 – 3167, 2010.

- [14] M. Fikri, J. Herzler, R. Starke, C. Schulz, P. Roth, and G. Kalghatgi. Autoignition of gasoline surrogates mixtures at intermediate temperatures and high pressures. *Combustion and Flame*, 152:276 – 281, 2008.
- [15] B. Gauthier, D. Davidson, and R. Hanson. Shock tube determination of ignition delay times in full-blend and surrogate fuel mixtures. *Combustion and Flame*, 139:300 – 311, 2004.
- [16] J. B. Heywood. *Internal Combustion Engine Fundamentals*. McGraw-Hill, New York, 1988.
- [17] M. Kraft, P. Maigaard, F. Mauss, M. Christensen, and B. Johansson. Investigation of combustion emissions in an HCCI engine – measurements and a new computational model. *Proceedings of the Combustion Institute*, 28:1195–1201, 2002.
- [18] T. Lu and C. Law. A directed relation graph method for mechanism reduction. *Proceedings of the Combustion Institute*, 156:1333 – 1341, 2005.
- [19] N. Marinov. A detailed chemical kinetic model for high temperature ethanol oxidation. *International Journal of Chemical Kinetics*, 30:183 – 220, 1999.
- [20] N. Morgan, A. Smallbone, A. Bhave, M. Kraft, R. Cracknell, and G. Kalghatgi. Mapping surrogate gasoline compositions into ron/mon space. *Combustion and Flame*, 157(6):1122–1131, 2010.
- [21] S. Mosbach, M. Kraft, A. Bhave, F. Mauss, J. H. Mack, and R. W. Dibble. Simulating a homogenous charge compression ignition engine fuelled with a DEE/EtOH blend. SAE Paper No. 2006-01-1362, 2006.
- [22] S. Mosbach, M. Celnik, R. Abijeet, M. Kraft, H. Zhang, S. Kubo, and K. Kim. Towards a detailed soot model for internal combustion engines. *Combustion and Flame*, 156:1156 – 1165, 2009.
- [23] K. Niemeyer and C. Sung. Mechanism reduction strategies for multicomponent gasoline surrogate fuels. 7th US National Combustion Meeting of the Combustion Institute, March 2011.
- [24] R. Niven. Ethanol in gasoline: environmental impacts and sustainability review article. *Renewable and Sustainable Energy Reviews*, 9:535 – 555, 2005.
- [25] S. B. Pope. PDF methods for turbulent reactive flows. *Progress in Energy and Combustion Science*, 11:119–192.
- [26] D. Sheen, C. Law, H. Wang, and T. Løvås. Spectral uncertainty quantification, propagation, and optimization of a detailed kinetic model for ethylene combustion. *Proceedings of the Combustion Institute*, 32:535 – 542, 2009.
- [27] R. Sivaramakrishnan, R. Tranter, and K. Brezinsky. High-pressure, high-temperature oxidation of toluene. *Combustion and Flame*, 139:340 – 350, 2004.



- [28] R. Sivaramakrishnan, R. Tranter, and K. Brezinsky. A high pressure model for the oxidation of toluene. *Proceedings of the Combustion Institute*, 30:1165 – 1173, 2005.
- [29] J. Smith, J. Simmie, and H. Curran. Autoignition of heptanes; experiments and modeling. *International Journal of Chemical Kinetics*, 37:728 – 736, 2005.
- [30] I. Sobol. On the systematic search in a hypercube. *SIAM Journal on Numerical Analysis*, 16(5):790 – 793, 1979.
- [31] A. Swarts and A. Yates. Insights into the role of autoignition during octane rating. SAE Paper No. 2007-01-0008, 2007.